General and Comparative Endocrinology 273 (2019) 40–51

Contents lists available at ScienceDirect

General and Comparative Endocrinology

journal homepage: www.elsevier.com/locate/ygcen

Research paper

Pituitary estrogen receptor alpha is involved in luteinizing hormone pulsatility at mid-gestation in the South American plains vizcacha, *Lagostomus maximus* (Rodentia, Caviomorpha)

Sofía Proietto[a,b], Lorena Yankelevich[a], Federico Martín Villarreal[a], Pablo Ignacio Felipe Inserra[a,b], Santiago Elías Charif[a,b], Alejandro Raúl Schmidt[a,b], Santiago Andrés Cortasa[a,b], María Clara Corso[a,b], Noelia Paula Di Giorgio[c], Victoria Lux-Lantos[c], Alfredo Daniel Vitullo[a,b], Julia Halperin[a,b], Verónica Berta Dorfman[a,b,*]

[a] Centro de Estudios Biomédicos, Biotecnológicos, Ambientales y Diagnóstico (CEBBAD), Universidad Maimónides, Ciudad Autónoma de Buenos Aires, Argentina
[b] Consejo Nacional de Investigaciones Científicas y Técnicas (CONICET), Argentina
[c] Laboratorio de Neuroendocrinología, Instituto de Biología y Medicina Experimental (IByME)-CONICET, Ciudad Autónoma de Buenos Aires, Argentina

ARTICLE INFO

Keywords:
Lagostomus maximus
Estrogen receptor
GnRH receptor
Luteinizing hormone
Pituitary gland

ABSTRACT

The South American plains vizcacha, *Lagostomus maximus*, is a caviomorph rodent native from Argentina, Bolivia and Paraguay. It shows peculiar reproductive features like pre-ovulatory follicle recruitment during pregnancy with an ovulatory process at around mid-gestation. We have described the activation of the hypothalamic – pituitary – ovarian (HPO) axis during pregnancy. A progressive decrease of progesterone (P4) at mid-pregnancy elicits the delivery of gonadotropin-releasing hormone (GnRH) with the consequent secretion of follicle stimulating hormone (FSH) and estradiol (E_2) followed by luteinizing hormone (LH) release resulting in follicular luteinization and the P4 concentration recover. Pituitary gland is the central regulator of the HPO axis being E_2 a key hormone involved in the regulation of its activity. In this work we analyzed the action of E_2 on the pituitary response to the GnRH wave as well as its involvement on LH secretion at mid-gestation in *L. maximus*. The expression of GnRHR at the pituitary pars distalis showed a significant decrease at mid-pregnancy compared to early- and term-gestating females. ERα showed a significant increment from mid-gestation whereas ERβ did not show variations throughout pregnancy; whereas the LH expression in the pituitary pars distalis showed a significant increase at mid-gestation, concordantly with serum LH, which was followed by a decrease at term-gestation with similar values than at early-pregnancy. The number of cells with co-localization of ERα and GnRHR showed a decline at mid-pregnancy related to early- and term-gestation, whereas the cells with co-localization of ERα and LH increased at mid- and term-pregnancy. On the other hand, *ex vivo* measuring of LH pulsatility showed a significant increment in the total mass of LH delivered at mid-pregnancy followed by a decrease at term-gestation. The stimulation of ERα with the PPT specific agonist induced a significant increment in the total mass of LH released, whereas no changes were determined when ERβ was stimulated with its specific agonist MPP. These results suggest that LH pulsatility rise at mid-pregnancy would be enabled by the increase of E_2 acting through ERα.

1. Introduction

The South American plains vizcacha, *Lagostomus maximus*, is a hystricognathe fossorial rodent that inhabits the Pampas region of Argentina extending up to the South of Paraguay and Bolivia (Jackson et al., 1996). The vizcacha exhibits several peculiar reproductive features that stand out from most mammalian species. This rodent is the major poly-ovulatory species so far described, with the ability to release up to 800 oocytes per estral cycle. Despite this extreme poly-ovulatory rate, only 8–12 fertilized oocytes are implanted in the uterine horns, and just one or two embryos are successfully gestated to term (Weir, 1971a,b). The gestation of vizcacha can be divided in different phases according to its endocrinologic environment (Dorfman et al., 2016; Fraunhoffer et al., 2017). A first phase of gestation that shows

* Corresponding author at: Centro de Estudios Biomédicos, Biotecnológicos, Ambientales y Diagnóstico (CEBBAD), Universidad Maimónides, Hidalgo 775 6to piso, C1405BCK, Ciudad Autónoma de Buenos Aires, Argentina.
E-mail address: dorfman.veronica@maimonides.edu (V.B. Dorfman).

https://doi.org/10.1016/j.ygcen.2018.04.001
Received 29 December 2017; Received in revised form 22 March 2018; Accepted 2 April 2018
Available online 12 April 2018

Table 1
Characteristics of each experimental group.

Experimental group	Time of capture	Number of embryos in uterus	Crown-heel length of foetuses (mm)	Estimated gestational age (number of days)**	Ovulatory Stigmata	E_2 levels (pg/ml)	LH levels (ng/ml)
Early pregnant (EP)	April	8–12	*10	25–35	no	21.3 ± 4.2	0.7 ± 0.2
Mid-pregnant (MP)	July	1–2	90–115	90–110	yes	85.6 ± 9.4	3.3 ± 0.6
Term-pregnant (TP)	August	1–2	145–156	144–154	no	30.1 ± 6.6	1.2 ± 0.2

*Size (mm) of implantation sites.
**Gestational age estimated according to Fraunhoffer et al. (2017).

increasing progesterone (P4) level that reaches its maximum at day 70 with the consequent inhibition of the HPO axis as seen in most mammals (Goodman et al., 1981; Scaramuzzi et al., 1971; Skinner et al., 1998). A second phase of gestation is characterized by a progressive P4 decrease from day 70 reaching its minimum level at day 100. In this phase, the embryos enter in a process of resorption that begins with those implanted proximally and progressively extends to the embryos implanted nearest the cervix that are still alive. A third phase occurs from day 100 until term with HPO axis activity. As P4 decreases, a significant increase in gonadotropin-releasing hormone (GnRH) delivery takes place, as well as increases in circulating follicle stimulating hormone (FSH) inducing pre-ovulatory follicle recruitment with high steroidogenic activity. This produces a significant increase of estradiol (E_2) followed by the surge of luteinizing hormone (LH) that induces follicle luteinization, without releasing the oocyte, but adding a considerable number of secondary corpora lutea that enable P4 concentration recovering. This key event rescues the still surviving distal foetuses that were not reached by the progressive resorption process initiated early after implantation, letting gestation coming to term (Weir, 1971a,b). The endocrinologic environment in the transition of second to third phase suggests the involvement of E_2 in the activity of the hypothalamus, as suggested by the increment of hypothalamic estrogen receptor α (ERα) (Inserra et al., 2017).

In general, ovulation results from the action of hypothalamic GnRH on its specific receptor (GnRHR) at adenohypophysis, which in turn activates FSH and LH delivery that act over follicular maturation and rupture, respectively (Abraham et al., 1972). A low-frequency of GnRH pulses favors the expression of the β subunit of FSH whereas a high-frequency of GnRH pulses promotes the expression of the β subunit of LH, differentially inducing the follicular phase or the luteal phase, respectively (Haisenleder et al., 1993). E_2, acting through its specific receptors (ERs), sensitizes the pituitary gland to GnRH resulting in stimulation of LH and FSH secretion (Fink, 1988; Freeman, 1988). Nuclear estrogen receptors isoforms ERα and ERB can activate transcription in response to estrogens (Kuiper et al., 1997; McInerney et al., 1998). Hypophyseal GnRHR expression could be regulated by different pathways involving the ER isoforms. Gonadotrophs express both ERα and ERB suggesting their interaction and autoregulation (Matsuda et al., 2002). The selective activation of ERα or ERβ is involved in the regulation of LH or FSH secretion respectively (Sánchez-Criado et al., 2002, 2004). However, in rats, ERα was shown to be the predominant isoform mediating pituitary E_2 effects (Mitchner et al., 1998; Vaillant et al., 2002).

In order to elucidate the role of E_2 on pituitary response to the GnRH surge at mid-gestation in *L. maximus* and its involvement on LH secretion to guarantee the HPO reactivation, we studied ERα, ERβ, GnRHR and LH expression and their localization in the pituitary gland throughout gestation. In addition, we evaluated LH pulsatility during pregnancy and its relation with ER isoforms.

2. Materials and methods

2.1. Animals

Adult female plains vizcachas [2.5–3.0Kg body weight; 2–2.5 years old determined by the dry crystalline lens weight, according to Jackson (1986)] were captured from a resident natural population at the Estación de Cría de Animales Silvestres (ECAS), Villa Elisa, Buenos Aires Province, Argentina, using live-traps located at the entrance of burrows. The capture and transport of animals were approved by the Ministry of Agriculture Authority of the Buenos Aires Province Government. All experimental protocols, as well as the handling and euthanasia procedures, were reviewed and approved by the Institutional Committee on the Use and Care of Experimental Animals (CICUAE) from Universidad Maimónides and conducted in accordance with the guidelines for the care and use of laboratory animals published by the National Institutes of Health (NIH, USA). In order to obtain females at different gestational stages, captures were planned according to the natural reproductive cycle as described by Llanos and Crespo (1952), and on our own previous expertise in the field (Charif et al., 2017; Dorfman et al., 2013; Fraunhoffer et al., 2017; Inserra et al., 2017; Jensen et al., 2006, 2008; Leopardo et al., 2011). Vizcachas were divided into three groups according to embryological and hormonal characteristics (Table 1): Early-pregnant females (EPf, N = 15), mid-pregnant females (MPf, N = 15), and term-pregnant females (TPf, N = 15). In addition, for estral cycle synchronization, non-pregnant females (N = 20) were captured in early-March before the beginning of the reproductive season. Animals were housed under a 12:12 h low-light cycle to simulate their natural luminal exposure (low light of 12 W followed by moon light) at 22 ± 2 °C constant room temperature, with food and tap water *ad libitum*.

2.2. Estral cycle synchronization treatment

Non-pregnant female vizcachas were injected intramuscularly with 250 IU/day of pregnant mare's serum gonadotropin (PMSG, Novormon 5000, Syntex, Argentina) during three consecutive days, followed by one intramuscular injection of 1000 IU of human chorionic gonadotropin (hCG, Ovusyn, Syntex, Argentina) at the fourth day as previously described (Charif et al., 2016). Animals were sacrificed 9 days after the first PMSG injection at an early luteal phase. The success of the ovulatory induction was corroborated by the presence of ovulatory stigmata at sacrifice.

2.3. Tissue collection

Animals were anaesthetized by the intramuscular injection of 13.5 mg/kg body weight ketamine chlorhydrate (Holliday Scott S.A., Buenos Aires, Argentina) and 0.6 mg/kg body weight xylazine chlorhydrate (Richmond Laboratories, Veterinary Division, Buenos Aires, Argentina). Animals were sacrificed by trained technical staff by an intracardiac injection of 0.5 ml/kg body weight of Euthanyl™ (sodium pentobarbital, sodium diphenilhidanthoine, Brouwer S.A., Buenos Aires, Argentina). Brains and pituitary glands were immediately removed. Isolated pituitary glands were either fixed in cold 4% neutral-buffered paraformaldehyde (PFA) (Sigma Aldrich Inc., St. Louis, Missouri, USA) for immunohistochemical studies, or incubated in Krebs-Ringer buffer for pulsatile studies, or neurohypophyses discarded and adenohypophyses quickly frozen and stored at −80 °C for Western-blot. Before performing euthanasia, blood samples were obtained by

cardiac puncture. In order to obtain homogenous groups, E_2 and LH serum levels were measured according to Inserra et al. (2017) confirming the inclusion of each animal into the study group (see Table 1).

2.4. Sodium dodecylsulphate polyacrylamide gel electrophoresis (SDS)-PAGE and Western-blotting

Adenohypophyses were homogenized (1:3 w/v) in RIPA buffer (0.1 M phosphate buffer saline (PBS) with 1% Igepal, 0.5% sodium deoxycolate and 0.1% SDS, pH 7.4), containing 0.1 μM aprotionin, 0.1 μM leupeptin, 0.1 μM pepstatin and 0.1 mM phenylmethylsulfonyl fluoride (PMSF). All procedures were carried out at 4 °C. Homogenates were centrifuged for 30 min at 14,000*g* and the supernatants collected. Protein concentration was determined by Bradford method (Bradford, 1976) using bovine serum albumin (BSA) as a standard. Equal amounts of solubilized proteins (40 μg) were mixed (4:1) with sample buffer (1M Tris-HCl with 10% w/v SDS, 30% v/v glycerol, 0.1% w/v bromophenol blue and 0.15% w/v 2-mercaptoethanol, pH 6.8) and heated for 3 min at 100 °C. Samples were separated on an SDS-polyacrylamide 10% running gel and 4% stacking gel (29:1 acrylamide:bis acrylamide, Bio-Rad Laboratories, Hercules, California, USA), with 0.25 M Tris-glycine, pH 8.3, as the electrolyte buffer, in an electrophoresis cell (Mini-PROTEAN II Electrophoresis Cell, Bio-Rad Laboratories, Hercules, California, USA). For Western-blot analysis, proteins were electro-transferred to a 0.2 mm polyvinylidene difluoride (PVDF) membrane (Immobilon-P, EMD Millipore Corporation, Billerica, Massachusetts, USA) at 250 mA for 2 h. For protein identification, membranes were blocked 1 h at room temperature with 5% powdered skim milk in PBS containing 0.1% Tween 20. Then, they were incubated overnight at 4 °C with the appropriate primary antibody (Table 2). Data normalization was performed by incubating the same membranes with anti-β-actin antibody (see Table 2). For immunoreactivity development, membranes were incubated with goat anti-rabbit IgG-HRP (1:3000 dilution, Bio-Rad Laboratories, Hercules, California, USA) or with goat anti-mouse IgG-HRP (1:3000 dilution, Bio-Rad Laboratories, Hercules, California, USA) as appropriate. For chemiluminiscence development, ECL Plus kit (GE Healthcare Ltd., Amersham Place, Buckinghamshire, United Kingdom) was employed. Membranes were scanned with a ImageQuant 350 Capture Imaging System (GE Healthcare Bio-Sciences AB, Uppsala, Sweden) and dot-blots analyzed with Image-Pro Plus software (Image-Pro Plus 6, Media Cybernetics Inc., Bethesda, Maryland, USA). The estimation of the band size was performed using a pre-stained protein ladder (PageRuler, Fermentas UAB, Vilnius, Lithuania) as molecular weight marker. Results were expressed as the ratio between the relative optical density (ROD) of the corresponding protein and the ROD of β-actin. Five animals per group were tested.

2.5. Immunohistochemistry

After removal, pituitary glands were fixed in cold 4% PFA in 0.1 M PBS (pH 7.4) for 48 h, dehydrated through a graded series of ethanol and embedded in paraffin. Pituitary glands were cut to serial coronal sections (5 μm thick) containing adeno- and neurohypophysis, and mounted onto coated slides. Sections were dewaxed in xylene, rehydrated through a decreasing series of ethanol (100%, 95% and 70%) and subjected to immunohistochemical assays. Antigen retrieval was performed by boiling sections in 10 mM sodium citrate buffer (pH 6) for 20 min, followed by 20 min of cooling at room temperature. Then, endogenous peroxidase activity was blocked with 2% hydrogen peroxide in methanol for 30 min. After that, sections were incubated with a blocking solution containing 10% normal serum in PBS (pH 7.4) for 1 h. Immunoreactivity was detected by incubating slides overnight at room temperature with a single primary antibody (see Table 2). Immunoreactivity was revealed with biotinylated goat anti-rabbit IgG or with biotinylated horse anti-mouse IgG followed by incubation with avidin-biotin complex (ABC Vectastain Elite kit, Vector Laboratories, Burlingame, California, USA) as appropriate. The reaction was visualized with 3,3′diaminobenzidine (DAB) and intensified with nickel ammonium sulphate (DAB kit, Vector Laboratories, Burlingame, California, USA) that yields a black product. For co-localization of ERα with LH or with GnRHR, a three-day step assay was performed. After revealing ERα antibody immunoreactivity with biotinylated goat anti-rabbit IgG with DAB plus nickel resulting in a black product as described above, sections were washed for 4 h with 2% Tween-PBS followed by overnight incubation with GnRHR antibody or LH antibody. Immunoreactivity was revealed with biotinylated horse anti-mouse IgG followed by incubation with avidin-biotin complex (ABC Vectastain Elite kit, Vector Laboratories, Burlingame, California, USA). The reaction was visualized with 3,3′diaminobenzidine (DAB) (DAB kit, Vector Laboratories, Burlingame, California, USA) that yields a brown product. The specificity of the assay was corroborated in adjacent sections by omission of the primary antibodies or by pre-absorption of the anti-ERα antibody with ERα blocking peptide (ERα(MC-20)P; Santa Cruz Biotechnology, Santa Cruz, CA, USA), or anti-LH antibody with Luteinizing Hormone β-Subunit (sc-358268; Santa Cruz Biotechnology, Santa Cruz, CA, USA). Blocking peptides were incubated overnight with their respective specific antibodies in a rotator at room temperature. Incubation was followed by centrifugation for 20 min at 15,000*g*. Finally, treated sections were dehydrated through a graded series of ethanol (70%, 95% and 100%), cleared in xylene (Merck KGaA, Darmstadt, Germany) and coverslipped. Five animals per group were tested.

2.6. Image analysis

Before assays, care was taken in selecting anatomically matching areas among animals. To determine the GnRHR, ERα and LH distribution, immunoreactive area (IRA) and antibodies co-localization, 3 slides with 3 pituitary sections per slide corresponding to rostral-end, medial and caudal-end regions were tested for each animal (5 animals per group). Adjacent sections were tested for each marker. At each section, three distinct adenohypophyseal fields were chosen avoiding superposition among them. Microscope images of immunoreactivity were captured with an optic microscope (BX40, Olympus Optical Corporation, Tokyo, Japan), fitted with a digital camera (390CU 3.2 Megapixel CCD Camera, Micrometrics, Spain), and the image software Micrometrics SE P4 (Standard Edition Premium 4, Micrometrics, Spain). All images were taken the same day under the same light condition to avoid external variations. Immunoreactive area was analyzed over the captured images using the Image Pro Plus software (Image Pro Plus 6, Media Cybernetics Inc, Bethesda Maryland, USA). Briefly, cells

Table 2
Used primary antibodies.

Target	IHQ dilution	WB dilution	Source	Company	Catalog
ERα	1:50	1:50	Rabbit	Santa Cruz Biotechnology Santa Cruz, USA	H-184, sc-7207
ERβ	1:200	1:300	Rabbit	Abcam Massachusetts, USA	ab3577
LH	1:200	1:200	Mouse	Biogenex Fremont, USA	AM030-5M
GnRHR	1:200	1:200	Mouse	Invitrogen New York, USA	A9E4, MA1-35383
β-actin	--------	1:6000	Mouse	Sigma-Aldrich Inc. St. Louis, Missouri, USA	AC-15, A5411
α-tubulin	--------	1:1000	Mouse	Santa Cruz Biotechnology Santa Cruz, USA	B-7, sc-5286

that had a gray level darker than a threshold criterion defined as the optic density three times higher than the mean background density were considered for the estimation. The mean background density was measured in a region devoided of specific immunoreactivity, immediately adjacent to the analyzed region. IRA was determined by measuring the area covered by threshold pixels (pixels with a gray level higher than the defined threshold density). The gray level of threshold setting was maintained for all studied sections that were incubated with the same antibody. For the co-localization of ERα with GnRHR or with LH shown as gray-black nucleus with brown cytoplasm, the number of immunoreactive cells for both antibodies was semi-quantitatively scored considering: one, two or three + symbols indicating low (1 to 5 co-localized cells per field), medium (6 to 15 co-localized cells per field) or high co-localization (> 15 co-localized cells per field), respectively. Adobe Photoshop CS5 software (Adobe Systems Inc.) was used for digital manipulation of brightness and contrast when preparing the shown images.

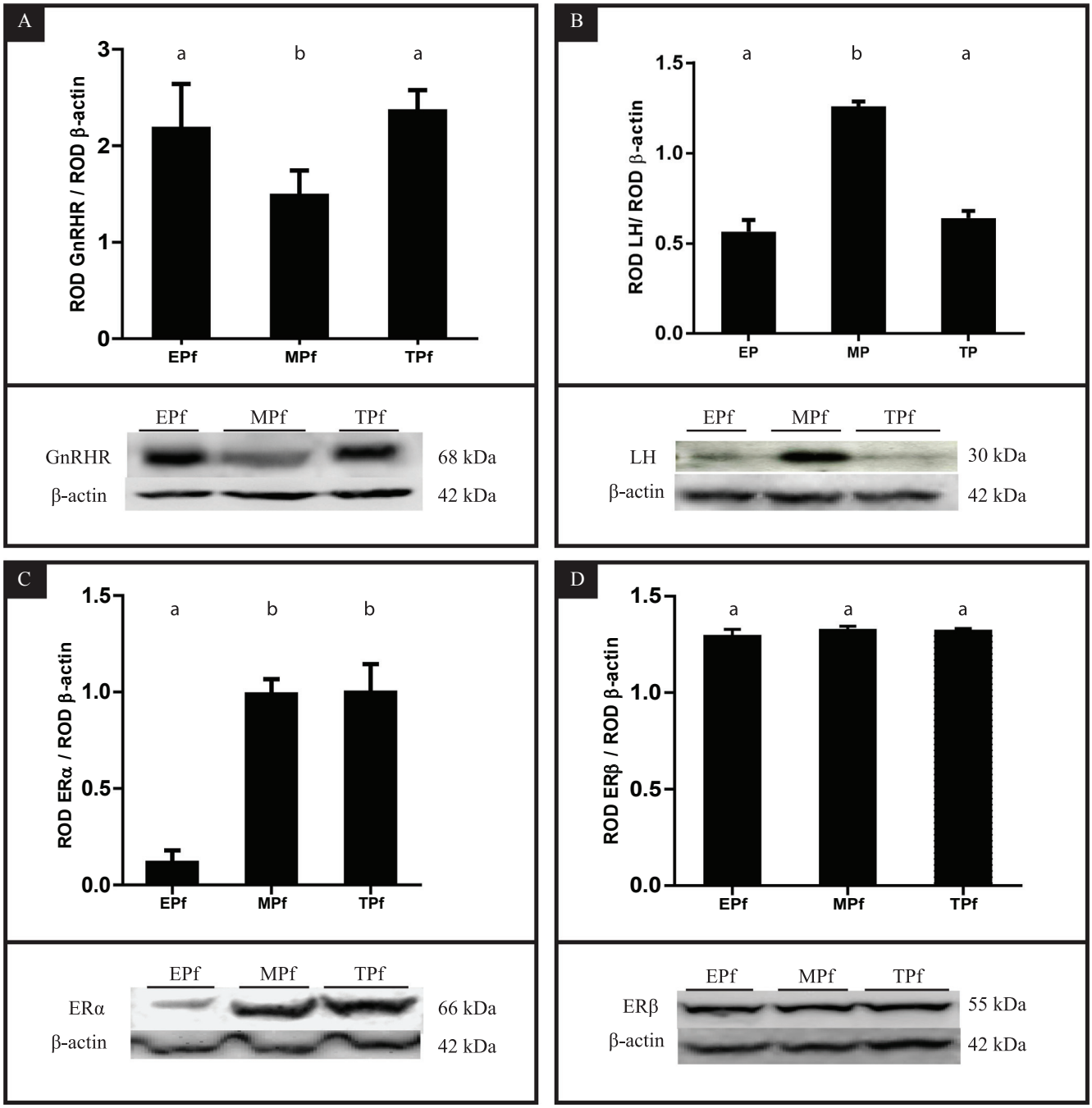

Fig. 1. Variation in GnRHR, LH, ERα and ERβ expression in pituitary gland of *Lagostomus maximus* throughout gestation. Adenohypophyseal protein expression of GnRHR, LH, ERα and Erβ was studied throughout pregnancy. A: Significant decrease of GnRHR was determined at mid-gestation with respect to early- and term-pregnancy. B: Significant increase of LH was determined at mid-gestation with respect to early- and term-pregnancy. C: Significant increase of ERα was observed in mid- and term-pregnancy related to early-gestation. D: No changes were depicted in ERβ expression during gestation. Representative images of respective dot-blot are shown under each graph. ANOVA followed by Newman-Keuls and Bonferroni's Multiple Comparison tests was employed to determine significant differences among groups. Different letters show significant differences with $p < 0.05$. EPf: early-pregnancy, MDf: mid-pregnancy, TPf: term-pregnancy, ROD: relative optical density.

2.7. LH pulsatility measured by radioimmunoassay (RIA)

LH pulsatility was measured *in vitro* as previously described for GnRH pulsatility (Charif et al., 2016). Pituitary glands of early-, mid- and term-pregnant animals, and of non-pregnant vizcachas in early luteal phase were evaluated. After sacrifice, whole pituitary glands were rapidly removed, weighed, placed in gelatin pre-coated tubes with 500 µl Krebs-Ringer buffer (115 mM NaCl, 4.7 mM KCl, 1.2 mM KH_2PO_4, 1.2 mM $MgSO_4$, 2.56 mM $CaCl_2$, and 20 mM $NaHCO_3$; pH 7.4) supplemented with 0.1% bovine serum albumin, 25 mM glucose and

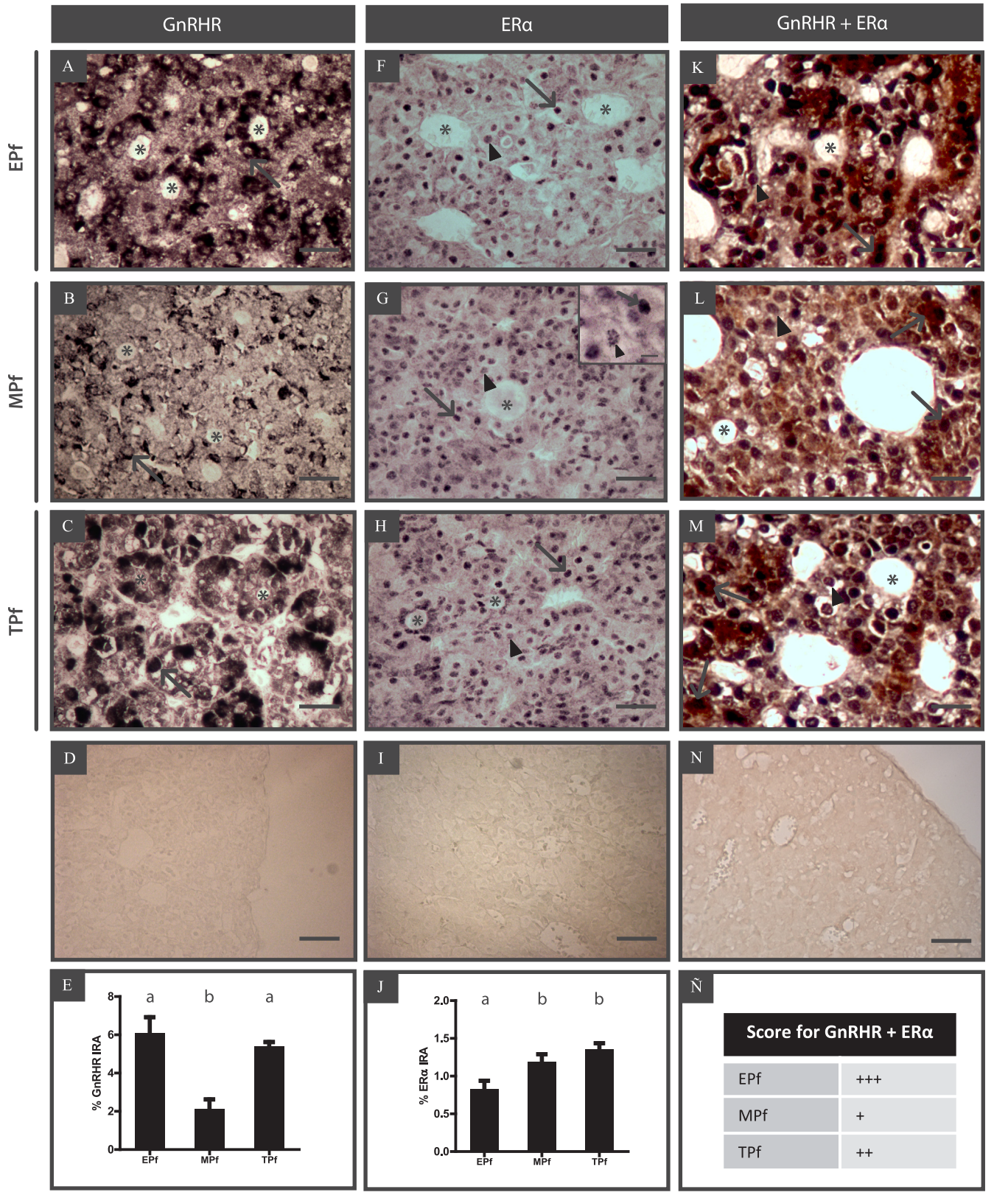

(caption on next page)

Fig. 2. GnRHR and ERα expression and distribution in the pars distalis of *Lagostomus maximus* during gestation. Expression of GnRHR and ERα was localized in the pars distalis of the pituitary gland throughout gestation. A–C: Cytoplasmic localization of GnRHR (arrows) in the pars distalis at early-, mid- and term-pregnancy. E: Significant decrease was determined in the GnRHR immunoreactive area at mid-gestation related to early- and term-pregnancy. F–H: Nuclear localization of ERα in the pars distalis at early-, mid- and term-pregnancy. Nuclei with weak (arrowhead) or strong (arrow) immunoreactivity were observed. J: Significant increase was determined in the ERα immunoreactive area at mid- and term-gestation with relation with early-pregnancy. K–M: Co-localization of GnRHR and ERα (arrows) was determined in the in the pars distalis at early-, mid- and term-pregnancy. Gonadotrophs with both cytoplasmic immunolocalization of GnRHR (brown) and nuclear immunoreactivity of ERα (gray-black) were observed in all the groups (arrows). In addition, some cells with nuclear ERα without GnRHR expression (arrowhead) were also detected. O: A score scale for GnRHR and ERα co-localization was performed. High quantity (+ + +) of cells with GnRHR and ERα co-localization was determined in early-gestation, low quantity (+) at mid-pregnancy, and mid-levels (+ +) of co-localization at term-gestation. D, I, N: Negative controls. Representative images are shown in all cases. E and J: ANOVA followed by Newman-Keuls and Bonferroni's Multiple Comparison tests was employed to determine significant differences among groups. Different letters show significant differences among groups with $p < 0.05$. EPf: early-pregnant females, MDf: mid-pregnant females, TPf: term-pregnant females, IRA: immunoreactive area, Asterisk (*): center of follicular structure. Scale bars: A–C and F–H = 40 μm, K–M = 20 μm, inset panel G = 8 μm, D, I and N = 80 μm.

16 mM HEPES buffer, and refrigerated for at least 1 h. Then, pituitary glands were preincubated in 500 μl of supplemented Krebs-Ringer buffer for 30 min at 37 °C, followed by 6 h incubation at 37 °C in fresh supplemented Krebs-Ringer buffer (pregnant and non-pregnant controls), or non-pregnant pituitary glands supplemented with PPT (hydroxyphenyl pyrazole, H6036, ERα agonist), MPP dihydrochloride hydrate (M7068, ERα antagonist), Way (WAY-200070, W1520, ERβ agonist), or Cyclo (Cyclofenil, C3490, ERβ antagonist), 10 μM each, all of them purchased to Sigma Aldrich Inc. (St. Louis, Missouri, USA) in the appropriated combinations: PPT + Cyclo, MPP + Way, and Cyclo + MPP. Selected concentrations of ERα and ERβ agonists and antagonists were based on previous works performed in rats, mice, ewes, and cancer cell lines (Arreguin-Arevalo et al., 2007; Clipperton-Allen et al., 2011; Hu et al., 2008; Kraichely et al., 2000; Lattrich et al., 2014; Serova et al., 2010). During incubation, the medium from each tube was collected at 7.5-min intervals, replaced with fresh medium and stored at −20 °C. A depolarizing concentration of potassium chloride (KCl, 100 mM) was added to the last tube (30 min) to test tissue viability by identifying a marked peak of LH release (not shown). LH content of each collected medium was determined by RIA with kits from the National Hormone and Pituitary Program, National Institute of Diabetes, Digestive and Kidney Diseases, USA. Results were expressed in terms of rat LH standards using the following standards: for LH iodination: r-LH-I10, reference preparation rat LH-RP-3 (AFP7187B) and anti-rat LH-S11 (AFPC697071P) (Catalano et al., 2010). Assay sensitivity was 0.31 ng/ml. Intra- and inter-assay coefficients of variation were 6.8% and 10.1%, respectively. A pooled pituitary homogenates of high LH content was serially diluted to prepare the vizcacha curve and the parallelism with the rat standard curve was confirmed, as previously described (Dorfman et al., 2013). LH pulsatile parameters were determined using the computer algorithm Cluster8 developed by Veldhuis and Johnson (1986) (Pulse_XP software, http://mljohnson.pharm.virginia.edu/home.html). A 2 × 2 cluster configuration and a *t*-statistic of 2 for the upstroke and down stroke, to maintain false-positive and false-negative error rates below 10%, were used as suggested by Martinez de la Escalera et al. (1992). Pituitary glands of five animals were tested per group.

2.8. Statistical analysis

Values are expressed as mean ± standard deviation (SD). All the experiments were performed by duplicate. Results were evaluated using *t*-test for comparisons between two groups, or one-way analysis of variance (ANOVA) followed by Newman-Keuls and Bonferroni's Multiple Comparison tests was employed for comparisons among more than two groups. Statistical analysis was performed using Prism 4.0 (GraphPad Software Inc., San Diego, California, USA). Differences were considered significant when $p < 0.05$.

3. Results

3.1. Variations in the expression of GnRHR, LH, ERα and ERβ during gestation

Predominant bands corresponding to the expected molecular weights were detected for GnRHR, LH, ERα and ERβ in pituitary glands of female vizcachas and female rat (Fig. 1, Supplementary material). In addition, negative controls were also evaluated for each antibody. A single band of 68 kDa was detected for GnRHR, 30 kDa for LH, 66 kDa for ERα, and 55 kDa for ERβ. An additional band of 46 kDa, previously described as REα isoform, was also observed. Furthermore, a heavier band of approximately 76 kDa, previously described for REα (Inserra et al., 2017) was also detected. The protein of muscle of vizcacha, used as a negative control, did not show reactive bands for any of the antibodies. This reproducible pattern between vizcachas and rat, as well as its absence in the negative controls, reinforces the specificity of the employed antibodies.

Protein expression of adenohypophyseal GnRHR changed during gestation with a significant decrease at mid-pregnancy related to early- and term-pregnancy (Fig. 1A). However, protein expression of LH showed a significant increment at mid-pregnancy followed by a decrease at term-gestation with similar values than early-pregnancy (Fig. 1B). Significant variation during gestation was also determined in ERα expression with increments in mid- and term-pregnant vizcachas (Fig. 1C); whereas, protein expression of ERβ did not change during gestation (Fig. 1D).

3.2. GnRHR and ERα expression and distribution in the pars distalis during gestation

Isolated cells, grouped cells and cells in the basal position of follicular structures, all of them showing GnRHR immunoreactivity, have been found in the pituitary pars distalis (Fig. 2A–C). A significant decrease in the total GnRHR immunoreactive area (IRA) was detected at mid-pregnancy compared to early- and term-pregnant animals (Fig. 2E). Nuclear ERα-immunoreactivity with a granular pattern was seen in isolated cells, grouped cells, or cells of follicular structures in the pituitary pars distalis. Nuclei with both weak and strong immunoreactivity were observed in all the studied animals independently of the gestation phase (Fig. 2F–H). A significant increase in the total immunoreactive area (IRA) at mid- and term-pregnancy was determined (Fig. 2J). In all the analyzed animals, almost all GnRHR immunoreactive cytoplasms showed co-localization with nuclear ERα; however, a few cells with nuclear ERα immunopositivity without cytoplasmic GnRHR immunosatining were also observed (Fig. 2 K-M). The score scale of the abundance of cells with GnRHR and ERα co-localization showed a decrease at mid-pregnancy with a recovery at term-gestation (Fig. 2O). This co-localization variation pattern was in

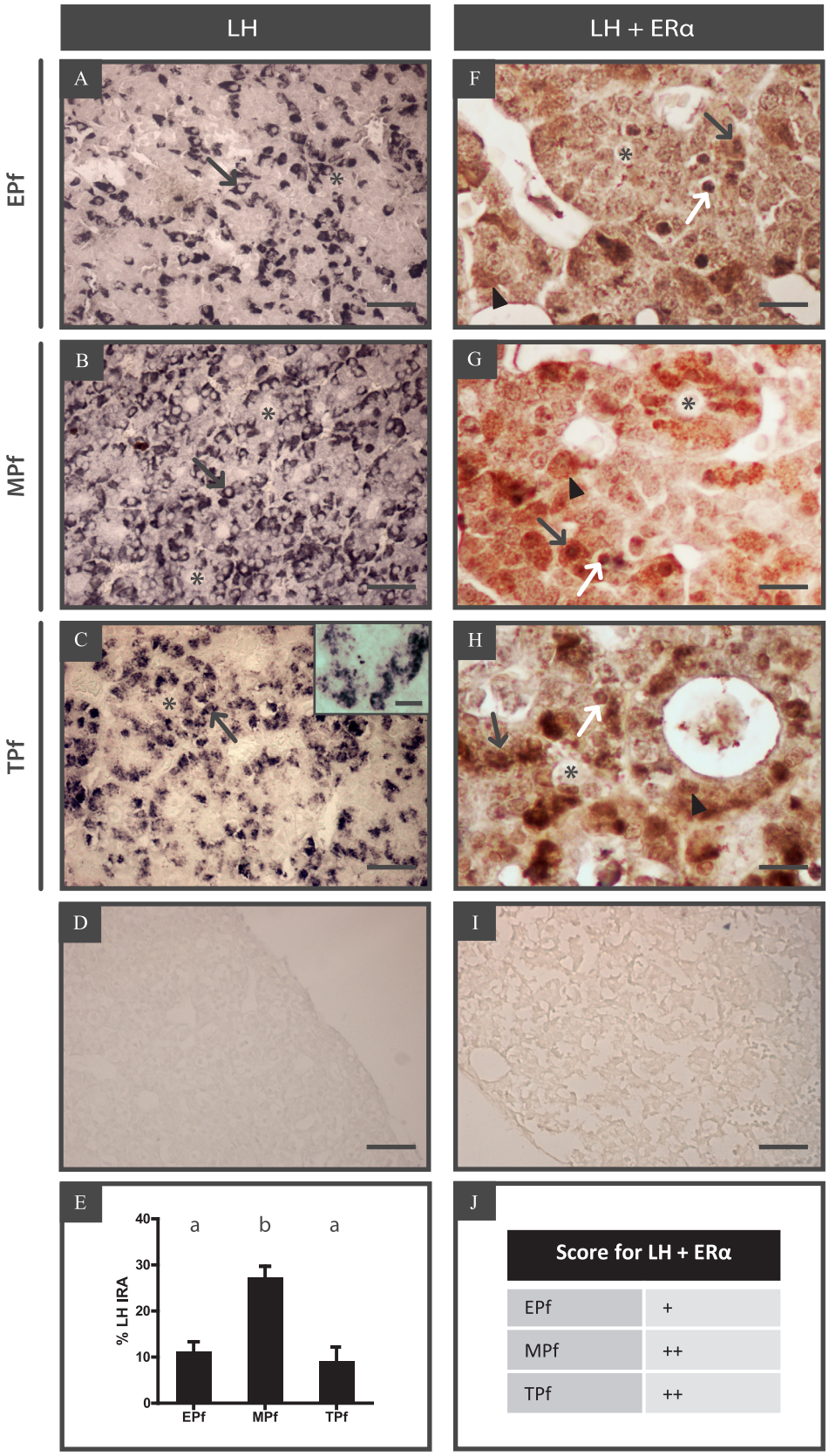

Fig. 3. LH and ERα expression and distribution in the pars distalis of *Lagostomus maximus* during gestation. Expression of LH and its co-localization with ERα in the pars distalis of the pituitary gland throughout pregnancy. A–C: Cytoplasmic localization of LH (arrows) in the pars distalis at early-, mid- and term-pregnancy. E: Significant increment at mid-gestation was determined in the LH immunoreactive area (IRA). ANOVA followed by Newman-Keuls and Bonferroni's Multiple Comparison tests was employed to determine significant differences among groups. Different letters show significant differences among groups with $p < 0.05$. F–H: Co-localization of LH and ERα was determined in the pars distalis at early-, mid- and term-pregnancy. Gonadotrophs with cytoplasmic immunolocalization of LH (brown) and nuclear immunoreactivity of ERα (gray-black) were observed in all the groups (arrows). In addition, a few gonadotrophs with LH immunoreactivity without ERα expression (arrowhead), and some cells with exclusively nuclear ERα immunopositivity (white arrow), were also detected. J: A score scale for LH and ERα co-localization was performed. Low number of cells (+) with LH and ERα co-localization was determined in early-pregnant females, whereas mid-levels (++) of co-localization were observed at mid-pregnant and term-pregnant females. D, I: Negative controls. Representative images are shown in all cases. EPf: early-pregnant females, MDf: mid-pregnant females, TPf: term-pregnant females. Asterisk (*): center of follicular structure. Scale bars: A–C = 50 μm, F–H = 15 μm, D and I = 80 μm.

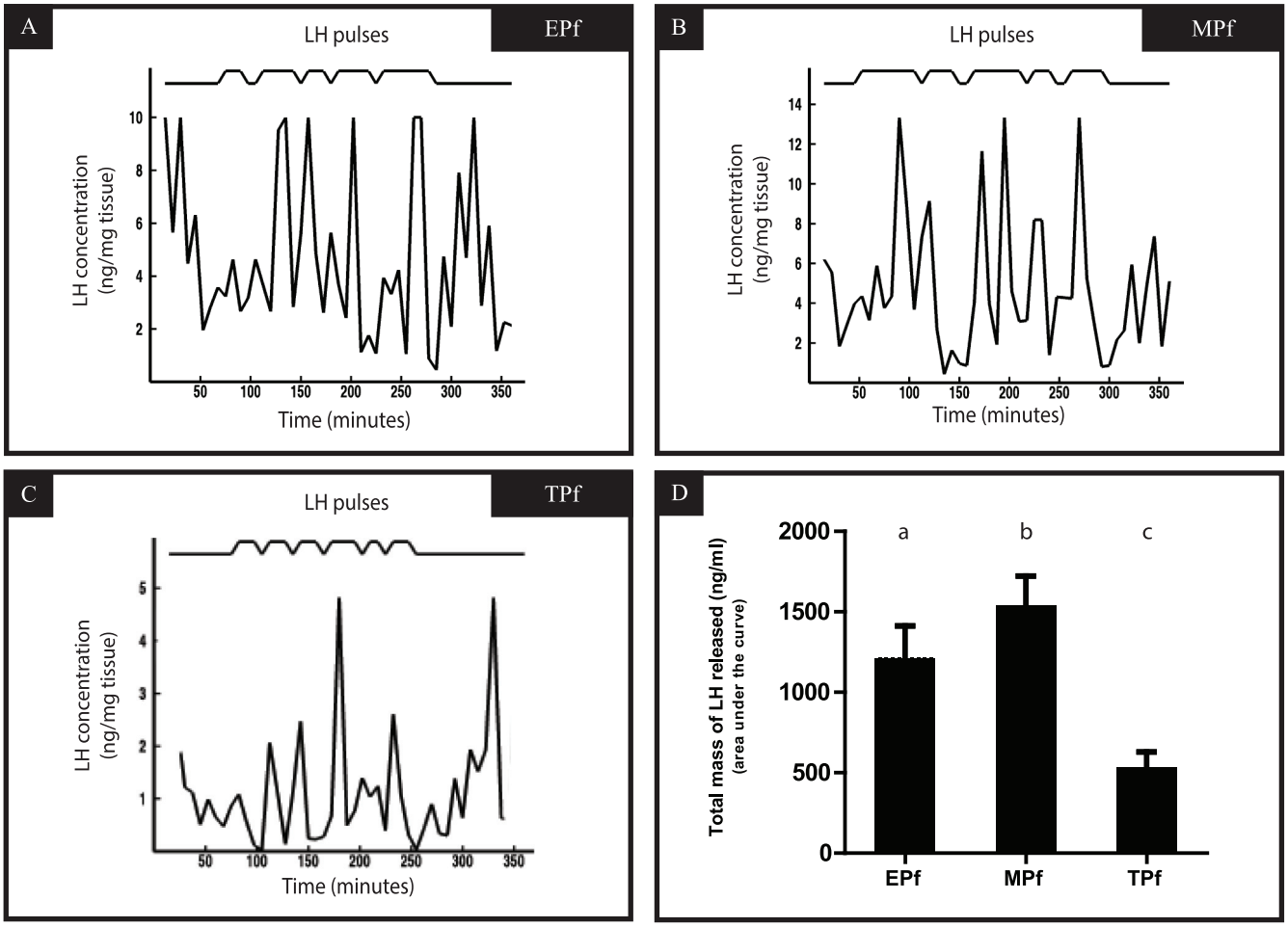

Fig. 4. Variations in LH pulsatility of *Lagostomus maximus* during gestation. A–C: Representative images of LH pulsatile pattern throughout gestation. The upper lines in the graphics indicate the pulses occurrence. Around 5 pulses of LH were observed without differences during pregnancy. A: Early-pregnant females (EPf). B: Mid-pregnant females (MPf). C: Term-pregnant females (TPf). D: Total mass of LH released during the assay. Significant changes were observed among groups with increase at mid-pregnancy and decrease at term-pregnancy. ANOVA followed by Newman-Keuls and Bonferroni's Multiple Comparison tests was employed to determine significant differences among groups. Different letters show significant differences with $p < 0.05$.

concordance with the GnRHR immunoreactive area (IRA) variation pattern observed throughout gestation (Fig. 2E). Negative controls did not reveal any staining in all examined sections (Fig. 2D, I, N).

3.3. LH and ERα expression and distribution in the pars distalis during gestation

Gonadotrophs with a cytoplasmic granular LH immunoreactive pattern were observed in the pituitary pars distalis of gestating vizcachas. Cells with LH immunoreactivity were found isolated, grouped or localized in the basal position of follicular structures (Fig. 3A–C). Significant variation in the total LH immunoreactive area (IRA) was detected throughout gestation with increase at mid-pregnancy and latter decrease at term-pregnancy up to early-pregnancy levels (Fig. 3E). Co-localization of cytoplasmic LH and nuclear ERα in the same cells was detected in all analyzed animals; however, cells with separately cytoplasmic LH or nuclear ERα immunoreactivity were also identified (Fig. 3F–H). The score scale of the abundance of cells with LH and ERα co-localization throughout gestation showed an increase at mid- and late-pregnancy (Fig. 3J). Negative controls did not reveal any staining in all examined sections (Fig. 3D, I).

3.4. Variations in LH pulsatility during gestation

Pituitary gland LH pulsatility was evaluated *ex vivo* throughout gestation. Around 5–6 pulses were observed during the experiment without significant differences among the three evaluated groups (Fig. 4A–C). However, the total mass of LH secreted showed significant variations throughout gestation with an increase at mid-pregnancy and a marked decrease at term-pregnancy (Fig. 4D).

3.5. LH pulsatility modulation by estrogen receptors

To evaluate the estrogen receptor isoform involved in LH pulsatility, the estrous cycle of non-pregnant vizcachas was synchronized (see Materials and Methods) and LH pulsatility *ex vivo* determined during six hours in pituitaries treated with agonists and antagonists of ERα and ERβ. A significant increment in the total mass of LH released was observed in pituitary glands incubated with the specific ERα agonist plus the ERβ antagonist (PPT + Cyclo). No changes were detected in the total mass of LH released when pituitary glands were treated with the agonist of ERβ plus the antagonist of ERα (MPP + Way), or with the both antagonists (Cyclo + Way) (Fig. 5A). In addition, no changes were determined in the frequency of LH pulses among groups (Fig. 5B–F).

4. Discussion

This work shows the key action of E_2 on LH delivery and demonstrates its participation in the HPO axis reactivation during gestation in the South American plains vizcacha. ERα variation throughout

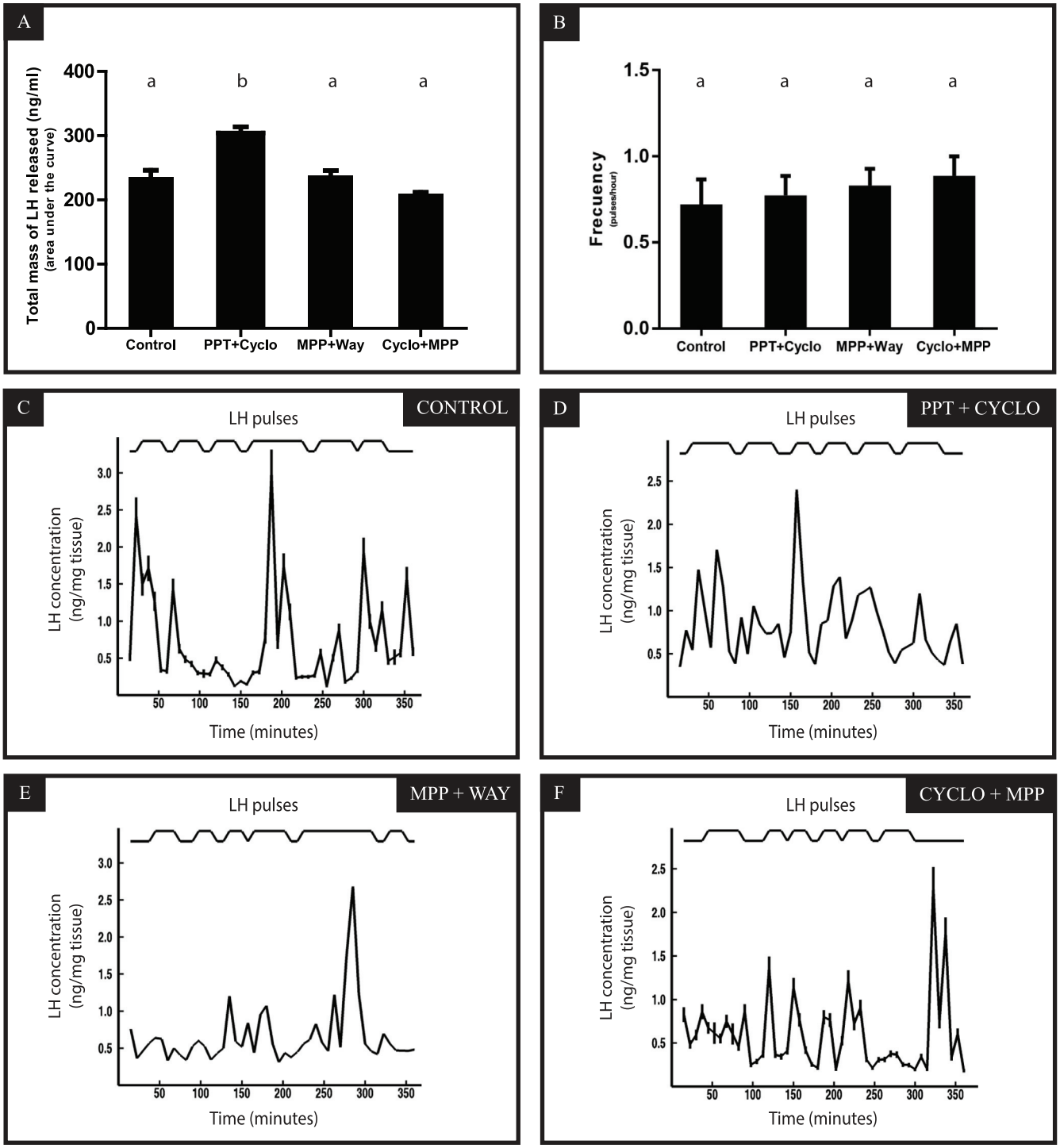

Fig. 5. Modulation of LH pulsatility by estrogen receptors in *Lagostomus maximus*. LH pulsatility is modulated by ERα. A: A significant increment in the total mass of LH released during the assay was observed when pituitaries were treated with the ERα agonist PPT together with the ERβ antagonist Cyclofenil. Differences were not determined when pituitaries were treated with the ERα antagonist MPP together with the ERβ agonist Way, or when both ER isoforms were blocked using both antagonists together. B: The frequency of LH pulses did not show significant differences among the evaluated treatments. ANOVA followed by Newman-Keuls and Bonferroni's Multiple Comparison tests was employed to determine significant differences among treatments. Different letters show significant differences with $p < 0.05$. C–F: Representative images of LH pulsatile pattern secreted by pituitary glands incubated with: Krebs-Ringer buffer (Control group, C), Krebs-Ringer buffer supplemented with ERα agonist and ERβ antagonist (PPT + Cyclo, D), Krebs-Ringer buffer supplemented with ERα antagonist and ERβ agonist (MPP + Way, E), Krebs-Ringer buffer supplemented with ERα antagonist and ERβ antagonist (Cyclo + MPP, F). Five to 6 pulses of LH were observed without significant differences among groups. The upper lines in the graphics indicate the pulses occurrence. PPT: hydroxyphenyl pyrazole, MPP: dihydrochloride hydrate, Way: WAY-200070, Cyclo: Cyclofenil.

gestation was determined and its involvement on the total mass of LH released during its pulsatility was proved.

The variation of hypophyseal ERα expression throughout pregnancy, with a significant increase since mid-gestation to term, and the constant levels of hypophyseal ERβ expression during pregnancy, suggest that ERα would be the predominant isoform modulating hypophyseal activity during the reproductive period. Similar results have been recently described in the hypothalamus of female vizcacha, where significant increments in ERα expression were observed at mid-gestation without variations in ERβ (Inserra et al., 2017). Considering that animals of the three analyzed gestation phases showed both weak and strong nuclear ERα immunoreactivity, the increment of ERα expression at mid- and term-gestation could result from a combined increment of the level of ERα expression and the number of ERα positive cells. In line with these observations, the sensitization of hypophysis to GnRH action resulting in LH, FSH and prolactin (PRL) secretion was observed in ovariectomized rats injected with the specific agonist of Erα, PPT (Sánchez-Criado et al., 2004). On the other hand, a culture of hypopyseal cells treated with GnRH showed increase in ERα mRNA (Demay et al., 1996) reinforcing ERα predominant involvement on gonadotrophs activation.

The concentration of GnRHR on the surface of the gonadotrophs is usually correlated with alterations in the response to GnRH availability (Marian et al., 1981). The relative amount of GnRHR observed during high frequency of GnRH pulses, which induces LH secretion, is two to three times higher than during low frequency pulses of GnRH that induces FSH release (Kaiser et al., 1995; Loumaye and Catt, 1982). Here, we found a significant decrease of both GnRHR immunoreactive area and GnRHR protein content in pars distalis of mid-pregnant vizcachas. Such evidence is opposed to the previously reported increment of hypothalamic GnRH in mid-gestating vizcachas (Dorfman et al., 2013; Inserra et al., 2017; Charif et al., 2017). This strongly indicates a mechanism of down regulation of hypophyseal GnRHR just after ovulation. The expression and distribution of GnRHR during pregnancy here described are similar to the previously described for other mammals like rats, heifers, and humans (Kadokawa et al., 2014; La Rosa et al., 2000; Marian and Conn, 1983).

Gonadotroph GnRHR expression is directly related with E_2. A two to three-fold increase in GnRHR was observed in gonadectomised rats, whereas replacement with sex steroids induced a significant GnRHR decay (Kaiser et al., 1993). Bearing in mind that mid-pregnant vizcachas show increased levels of E_2, the decrease in GnRHR expression and in its colocalization with ERα at mid-gestation also seems a consequence of the steroid increment. A similar decrease of GnRHR was observed in the αT3-1 cell line after treatment with estradiol (Weiss et al., 2006). However, Lerrant et al. (1995) showed that GnRHR mRNA is stimulated by E_2. Certainly, several factors should coincide to obtain the final regulation.

The expression and distribution of ERα in the hypophysis has been previously described in several mammals such as mouse (*Mus musculus)*, rat (*Rattus norvegicus),* sheep (*Ovis aries*), and cow (*Bos taurus*) (Lane et al., 2009; Pelletier et al., 2000; Polkowska et al., 2004; Sánchez-Criado et al., 2005, 2012). The detection of nuclear localization of ERα in cells of the pituitary pars distalis of vizcachas during pregnancy points to ERα acting as a transcription factor. The increment in the number of hypophyseal cells with co-localization of ERα and LH at mid- and term-pregnancy may indicate its involvement on LH expression and/or delivery. However, ERα immunoreactivity was also observed in cells without LH localization suggesting the involvement of ERα in other functions besides from the one it has in gonadotrophs. In rats, ERα is expressed at high levels in lactotrophs and gonadotrophs (Keefer et al., 1976; Mitchner et al., 1998). The ERα expression in immunonegative LH and GnRHR cells of the pituitary glands of vizcacha may indicate its involvement in lactotrophs activity. On the other hand, the detection of ERβ in the cell cytoplasm of pituitary glands of pregnant vizcachas (data not shown), together with the constant levels of hypophyseal ERβ expression observed during pregnancy, suggest that ERβ would not be acting on the modulation of pituitary function during gestation. A careful insight should be done into ERβ results considering that there are currently no fully reliable commercial antibodies (Snyder et al., 2010). However, the antibody employed in the present work seems to be specific for hypophyseal ERβ since we detected a single band for ERβ in the pituitary gland of rat and vizcacha in the Western-blot assay.

Cytoplasmic localization of LH in gonadotrophs of the pituitary pars distalis of vizcacha, with histological and morphometric changes during pregnancy, probably related to the requirements of this physiological stage, have been previously described (Filippa et al., 2005, 2012; Filippa and Mohamed, 2010). Here, we observed vesicular distribution of LH in pituitary gonadotrophs and confirmed the previously reported variation of the LH immunoreactive area in the pars distalis throughout gestation as well as in the LH hypophyseal content determined by Western-blot. Nevertheless, a significant increase in the total mass of LH released at mid-pregnancy was determined in the pulsatile studies, without changes in frequency, and this increment in the secretory pattern was concordant with the increased levels of serum LH showed by these animals (Dorfman et al., 2013; Fraunhoffer et al., 2017). All together, these determinations could indicate that the stored and newly synthetized LH is rapidly delivered at mid-gestation in order to induce ovulation and luteinisation. In addition, LH and prolactin would interact in the modulation of development and steroidogenic activity of accessory corpus luteum in the pregnant vizcacha maintaining E_2 and P4 secretion up to parturition as described in mouse (Clarke and Brook, 2001; Devi and Halperin, 2014).

In this work we described for the first time the basal pulsatile pattern of LH in pregnant and non-pregnant female vizcachas. Pregnant and non-pregnant animals with an early luteal phase showed a pulsatile pattern of around five to six pulses during 6 h. This pattern is concordant with the GnRH pulsatile pattern recently described in vizcachas in early luteal phase (Charif et al., 2016). Moreover, we showed an increment in the total mass of LH secreted as result of the action of the specific ERα agonist PPT, whereas the treatment of pituitaries with the specific ERβ agonist MPP, or with the combination of both ER isoforms specific antagonists Cyclofenil and MPP, showed similar values than the control treatment. These results may indicate the involvement of ERα isoform in LH secretion.

In conclusion, the results showed in this work suggest that the increment in LH pulsatility at mid-pregnancy would be enabled by the increase of ovarian E_2 at this point acting in gonadotrophs through ERα.

Acknowledgments

This work was supported by CONICET – Argentina (PIP N° 110/14), MINCyT – Argentina (PICT1281/2014), and by Fundación Científica Felipe Fiorellino, Universidad Maimónides, Argentina. We are especially grateful to the Ministerio de Asuntos Agrarios, Dirección de Flora y Fauna, Buenos Aires Province for enabling animal capture, to the personnel of ECAS for their invaluable help in trapping and handling the animals, to MV. Sergio Ferraris and MV. Fernando Lange and their veterinarian staff for their assistance for vizcachas handling and anesthetizing, and to Ms. Sol Clausi Schettini for her technical assistance in tissue processing.

Appendix A. Supplementary data

Supplementary data associated with this article can be found, in the online version, at http://dx.doi.org/10.1016/j.ygcen.2018.04.001.

References

Abraham, G.E., Odell, W.D., Swerdloff, R.S., Hopper, K., 1972. Simultaneous radioimmunoassay of plasma FSH, LH, progesterone, 17-hydroxyprogesterone and estradiol-17β during the menstrual cycle. J. Clin. Endocrinol. Metab. 34, 312–318.

Arreguin-Arevalo, J.A., Davis, T.L., Nett, T.M., 2007. Differential modulation of gonadotropin secretion by selective estrogen receptor 1 and estrogen receptor 2 agonists in ovariectomized ewes. Biol. Reprod. 77, 320–328.

Bradford, M.M., 1976. Rapid and sensitive method for the quantitation of microgram quantities of protein utilizing the principle of protein-dye binding. Anal. Biochem. 72, 248–254.

Catalano, P.N., Di Giorgio, N., Bonaventura, M.M., Bettler, B., Libertun, C., Lux-Lantos, V.A., 2010. Lack of functional GABA(B) receptors alters GnRH physiology and sexual dimorphic expression of GnRH and GAD-67 in the brain. Am. J. Physiol. Endocrinol. Metab. 298, E683–E696.

Charif, S.E., Inserra, P.I.F., Di Giorgio, N.P., Schmidt, A.R., Lux-Lantos, V., Vitullo, A.D., Dorfman, V.B., 2016. Sequence analysis, tissue distribution and molecular physiology of the GnRH preprogonadotrophin in the South American plains vizcacha (*Lagostomus maximus*). Gen. Comp. Endocrinol. 232, 174–184.

Charif, S.E., Inserra, P.I.F., Schmidt, A.R., Di Giorgio, A.P., Cortasa, S.A., Gonzalez, C.R., Lux-Lantos, V., Halperin, J., Vitullo, A.D., Dorfman, V.B., 2017. Local production of neurostradiol affects gonadotropin-releasing hormone (GnRH) secretion at mid-gestation in *Lagostomus maximus* (Rodentia, Caviomorpha). Physiol. Rep. 5, e13439.

Clarke, J., Brook, F., 2001. Effect of gonadotrophins on the ovarian interstitial tissue of the wood mouse *Apodemus sylvaticus*. Reproduction 121 (1), 123–129.

Clipperton-Allen, A.E., Almey, A., Melichercik, A., Allen, C.P., Choleris, E., 2011. Effects of an estrogen receptor alpha agonist on agonistic behaviour in intact and gonadectomized male and female mice. Psychoneuroendocrinology 36, 981–995.

Demay, F., Tiffoche, C., Thieulant, M.L., 1996. Sex-and cell-specific expression of an estrogen receptor isoform in the pituitary gland. Neuroendocrinology 63, 522–529.

Devi, Y.S., Halperin, J., 2014. Reproductive actions of prolactin mediated through short and long receptor isoforms. Mol. Cell. Endocrinol. 382 (1), 400–410.

Dorfman, V.B., Saucedo, L., Di Giorgio, N.P., Inserra, P.I.F., Fraunhoffer, N., Leopardo, N.P., Halperin, J., Lux-Lantos, V., Vitullo, A.D., 2013. Variation in progesterone receptors and GnRH expression in the hypothalamus of the pregnant South American plains vizcacha, *Lagostomus maximus* (Mammalia, Rodentia). Biol. Reprod. 89 (5), 115–125.

Dorfman, V.B., Inserra, P.I.F., Leopardo, N.P., Halperín, J., Vitullo, A.D., 2016. The South American plains vizcacha, *Lagostomus maximus*, as a valuable animal model for reproductive studies. JSM. Anat. Physiol. 1 (1), 1004.

Filippa, V., Mohamed, F., 2010. The pituitary of non-pregnant and pregnant viscachas (*Lagostomus maximus maximus*): a comparative study by immunohistochemistry and morphometric analysis. Zoology 113, 361–372.

Filippa, V., Penissi, A., Mohamed, F., 2005. Seasonal variations of gonadotropins in the pars distalis male viscacha pituitary. Effect of chronic melatonin treatment. Eur. J. Histochem. 49, 291–300.

Filippa, V., Acosta, M., Mohamed, F., 2012. Cellular associations of pituitary gonadotrophs in a rodent (*Lagostomus maximus maximus*) with photoperiod-dependent reproduction. Tissue Cell 44, 351–357.

Fink, G., 1988. Gonadotropin secretion and its control. In: Knobil, E., Neill, J. (Eds.), The Physiology of Reproduction. Raven Press, New York, pp. 1349–1377.

Fraunhoffer, N.A., Jensen, F., Leopardo, N.P., Inserra, P.I.F., Meilerman Abuelafia, A., Dorfman, V.B., Vitullo, A.D., 2017. Hormonal behavior correlates with follicular recruitment at mid-gestation in the South American plains vizcacha *Lagostomus maximus*. Gen. Comp. Endocrinol. 250, 162–174.

Freeman, M.E., 1988. The ovarian cycle of the rat. In: Knobil, E., Neill, J. (Eds.), The Physiology of Reproduction. Raven Press, New York, pp. 1893–1928.

Goodman, R.L., Bittman, E.L., Foster, D.L., Karsch, F.J., 1981. The endocrine basis of the synergistic suppression of luteinizing hormone by estradiol and progesterone. Endocrinology 109, 1414–1417.

Haisenleder, D.J., Ortolano, G.A., Yasin, M., Dalkin, A.C., Marshall, J.C., 1993. Regulation of gonadotropin subunit messenger ribonucleic acid expression by gonadotropin-releasing hormone pulse amplitude in vitro. Endocrinology 132, 1292–1296.

Hu, L., Gustofson, R.L., Feng, H., Leung, P.K., Mores, N., Krsmanovic, L.Z., Catt, K.J., 2008. Converse regulatory functions of estrogen receptor-α and –β subtypes expressed in hypothalamic gonadotropin-releasing hormone neurons. Mol. Endocrinol. 22 (10), 2250–2259.

Inserra, P.I.F., Charif, S.E., Di Giorgio, N.P., Saucedo, L., Schmidt, A.R., Fraunhoffer, N., Halperin, J., Leopardo, N.P., Halperin, J., Lux-Lantos, V., Gonzalez, C.R., Vitullo, A.D., Dorfman, V.B., 2017. ERα and GnRH co-localize in the hypothalamic neurons of the South American plains vizcacha, *Lagostomus maximus* (Rodentia, Caviomorpha). J. Mol. Histol. 48 (3), 259–273.

Jackson, J.E., 1986. Determinación de edad en la vizcacha (*Lagostomus maximus*) en base al peso del cristalino. Vida. Silv. Neotrop. 1, 41–44.

Jackson, J.E., Branch, L.C., Villarreal, D., 1996. *Lagostomus maximus*. Mamm. Species 543, 1–6.

Jensen, F., Willis, M.A., Albamonte, M.S., Espinosa, M.B., Vitullo, A.D., 2006. Naturally suppressed apoptosis prevents follicular atresia and oocyte reserve decline in the adult ovary of *Lagostomus maximus* (Rodentia, Caviomorpha). Reproduction 132, 301–308.

Jensen, F., Willis, M.A., Leopardo, N.P., Espinosa, M.B., Vitullo, A.D., 2008. The ovary of the gestating South American plains vizcacha (*Lagostomus maximus*): suppressed apoptosis and corpora lutea persistence. Biol. Reprod. 79, 240–246.

Kadokawa, H., Pandey, K., Nahar, A., Nakamura, U., Rudolf, F.O., 2014. Gonadotropin-releasing hormone (GnRH) receptors of cattle aggregate on the surface of gonadotrophs and are increased by elevated GnRH concentrations. Anim. Reprod. Sci. 150, 84–95.

Kaiser, U.B., Jakubowink, A., Steinberger, A., Chin, W.W., 1993. Regulation of rat pituitary gonadouopin-releasing hormone receptor mRNA levels in vivo and in vitro. Endocrinology 133, 931–934.

Kaiser, U.B., Sabbagh, E., Katzenellenbogen, R.A., Conn, P.M., Chin, W.W., 1995. A mechanism for the differential regulation of gonadotropin subunit gene expression by gonadotropin-releasing hormone. Proc. Natl. Acad. Sci. U.S.A. 92, 12280.

Keefer, D.A., Stumpf, W.E., Petrusz, P., 1976. Quantitative autoradiographic assessement of ^{3}H-estradiol uptake in immunocytochemically characterized pituitary cells. Cell Tissue Res. 166, 25–35.

Kraichely, D.M., Sun, J., Katzenellenbogen, J.A., Katzenellenbogen, B.S., 2000. Conformational changes and coactivator recruitment by novel ligands for estrogen receptor-α and Estrogen receptor-β: correlations with biological character and distinct differences among SRC coactivator family members. Endocrinology 141 (10), 3534–3545.

Kuiper, G.G., Carlsson, B., Grandien, K., Enmark, E., Haggblad, J., Nilsson, S., Gustafsson, J.-A., 1997. Comparison of the ligand binding specificity and transcript tissue distribution of estrogen receptors α and β. Endocrinology 138, 863–870.

La Rosa, S., Celato, N., Uccella, S., Capella, C., 2000. Detection of gonadotropin-releasing hormone receptor in normal human pituitary cells and pituitary adenomas using immunohistochemistry. Virchows Archiv. 437, 264–269.

Lane, E.A., Sweeney, T., Ryan, M., Roche, J.F., Crowe, M.A., 2009. Relationship between serum gonadotropins and pituitary immunoreactive gonadotropins and steroid receptors during the first FSH increase of the estrous cycle and following steroid treatment in heifers. Anim. Reprod. Sci. 112 (1–2), 66–82.

Lattrich, C., Schüler, S., Häring, J., Skrzypczak, M., Ortmann, O., Treeck, O., 2014. Effects of a combined treatment with tamoxifen and estrogen receptor β agonists on human breast cancer cell lines. Arch. Gynecol. Obstet. 289 (1), 163–171.

Leopardo, N.P., Jensen, F., Willis, M.A., Espinosa, M.B., Vitullo, A.D., 2011. The developing ovary of the South American plains vizcacha, *Lagostomus maximus* (Mammalia, Rodentia): massive proliferation with no sign of apoptosis-mediated germ cell attrition. Reproduction 141, 633–641.

Lerrant, Y., Kottler, M.L., Bergametti, F., Moumni, M., Blumberg-Tick, J., Counis, R., 1995. Expression of gonadotropin-releasing hormone (GnRH) receptor gene is altered by GnRH agonist desensitization in a manner similar to that of gonadotropin beta-subunit gene in normal and castrated rat pituitary. Endocrinology 136, 2803–2808.

Llanos, A.C., Crespo, J.A., 1952. Ecología de la vizcacha (*Lagostomus maximus maximus* Blainv.) en el nordeste de la Provincia de Entre Ríos. Rev. Invest. Agrícolas. 6, 289–378.

Loumaye, E., Catt, K.J., 1982. Homologous regulation of gonadotropin-releasing hormone receptors in cultured pituitary cells. Science 215 (4535), 983–985.

Marian, J., Conn, P.M., 1983. Subcellular localization of the receptor for gonadotropin-releasing hormone in pituitary and ovarian tissue. Endocrinology 112 (1), 104–112.

Marian, J., Cooper, R.L., Conn, P.M., 1981. Regulation of the rat pituitary gonadotropin-releasing hormone receptor. Mol. Pharmacol. 19 (3), 399–405.

Martinez de la Escalera, G., Choi, A.L., Weiner, R.I., 1992. Generation and synchronization of gonadotropin-releasing hormone (GnRH) pulses: intrinsic properties of the GT1-1 GnRH neuronal cell line. Proc. Natl. Acad. Sci. U.S.A. 89, 1852–1855.

Matsuda, K.I., Ochiai, I., Nishi, M., Kawata, M., 2002. Colocalization and ligand-dependent discrete distribution of the estrogen receptor (ER) α and ERβ. Mol. Endocrinol. 16 (10), 2215–2230.

McInerney, E.M., Weis, K.E., Sun, J., Mosselman, S., Katzenellenbogen, B.S., 1998. Transcription activation by the human estrogen receptor subtype β (ERβ) studied with ERβ and ERα receptor chimeras. Endocrinology 139, 4513–4522.

Mitchner, N.A., Garlick, C., Ben-Jonathan, N., 1998. Cellular distribution and gene regulation of estrogen receptors alpha and beta in the ratpituitary gland. Endocrinology 139 (9), 3976–3983.

NIH, 1985. National Institutes of Health. Health Research Extension Act of 1985, Public Law 99-158. Animals in Research. Office of Laboratory Animal Welfare.

Pelletier, G., Labrie, C., Labrie, F., 2000. Localization of oestrogen receptor alpha, oestrogen receptor beta and androgen receptorsin the rat reproductive organs. J. Endocrinol. 165 (2), 359–370.

Polkowska, J., Ridderstråle, Y., Wańkowska, M., Romanowicz, K., Misztal, T., Madej, A., 2004. Effects of intracerebroventricular infusion of genistein on gonadotrophin subunit mRNA and immunoreactivity of gonadotrophins and oestrogen receptor-alpha in the pituitary cells of the anoestrous ewe. J. Chem. Neuroanat. 28 (4), 217–224.

Sánchez-Criado, J.E., Guelmes, P., Bellido, C., Gónzalez, M., Hernández, G., Aguilar, R.,

Garrido-Gracia, J.C., Bello, A.R., Alonso, R., 2002. Tamoxifen but not other selective estrogen receptor modulators antagonizes estrogen actions on luteinizing hormone secretion while inducing gonadotropin-releasing hormone self-priming in the rat. Neuroendocrinology 76 (4), 203–213.

Sánchez-Criado, J.E., de Las Mulas, J.M., Bellido, C., Tena-Sempere, M., Aguilar, R., Blanco, A., 2004. Biological role of pituitary estrogen receptors ERalpha and ERbeta on progesterone receptor expression and action and on gonadotropin and prolactin secretion in the rat. Neuroendocrinology 79 (5), 247–258.

Sánchez-Criado, J.E., de Las Mulas, J.M., Bellido, C., Aguilar, R., Garrido-Gracia, J.C., 2005. Gonadotrope oestrogen receptor-alpha and -beta and progesterone receptor immunoreactivity after ovariectomy and exposure to oestradiol benzoate, tamoxifen or raloxifene in the rat: correlation with LH secretion. J. Endocrinol. 184 (1), 59–68.

Sánchez-Criado, J.E., Trudgen, K., Millán, Y., Blanco, A., Monterde, J., Garrido-Gracia, J.C., Gordon, A., Aguilar, R., de Las Mulas, J.M., Ko, C., 2012. Estrogen receptor (ESR) 2 partially offsets the absence of ESR1 in gonadotropes of pituitary-specific Esr1 knockout female mice. Reproduction 143 (4), 549–558.

Scaramuzzi, R.J., Tillson, S.A., Thorneycroft, I.H., Caldwell, B.V., 1971. Action of exogenous progesterone and estrogen on behavioral estrus and luteinizing hormone levels in the ovariectomized ewe. Endocrinology 88, 1184–1189.

Serova, L.I., Harris, H.A., Maharjan, S., Sabban, E.L., 2010. Modulation of responses to stress by estradiol benzoate and selective estrogen receptor agonists. J. Endocrinol. 205 (3), 253–262.

Skinner, D.C., Evans, N.P., Delaleu, B., Goodman, R.L., Bouchard, P., Caraty, A., 1998. The negative feedback actions of progesterone on gonadotropinreleasing hormone secretion are transduced by the classical progesterone receptor. Proc. Natl. Acad. Sci. 95, 10978–10983.

Snyder, M.A., Smejkalova, T., Forlano, P.M., Woolley, C.S., 2010. Multiple ERbeta antisera label in ERbeta knockout and null mouse tissues. J. Neurosci. Methods 188, 226–234.

Vaillant, C., Chesnel, F., Schausi, D., Tiffoche, C., Thieulant, M.L., 2002. Expression of estrogen receptor subtypes in rat pituitary gland during pregnancy and lactation. Endocrinology 143 (11), 4249–4258.

Veldhuis, J.D., Johnson, M.L., 1986. Cluster analysis: a simple, versatile, and robust algorithm for endocrine pulse detection. Am. J. Physiol. Endocrinol. Metab. 250 (4), E486–E493.

Weir, B.J., 1971a. The reproductive organs of the female plains viscacha, *Lagostomus maximus*. J. Reprod. Fertil. 25, 365–373.

Weir, B.J., 1971b. The reproductive physiology of the plains viscacha, *Lagostomus maximus*. J. Reprod. Fertil. 25, 355–363.

Weiss, J.M., Polack, S., Treeck, O., Diedrich, K., Ortmann, O., 2006. Regulation of GnRH I receptor gene expression by the GnRH agonist triptorelin, estradiol, and progesterone in the gonadotroph-derived cell line alphaT3-1. Endocrine 30 (1), 139–144.